THE JOURNAL OF PHYSICAL CHEMISTRY B

Article

pubs.acs.org/JPCB

Water Dynamics in Divalent and Monovalent Concentrated Salt Solutions

Chiara H. Giammanco, Daryl B. Wong, and Michael D. Fayer*

Department of Chemistry, Stanford University, Stanford, California 94305, United States

ABSTRACT: Water hydrogen bond dynamics in concentrated salt solutions are studied using polarization-selective IR pump−probe spectroscopy and 2D IR vibrational echo spectroscopy performed on the OD hydroxyl stretching mode of dilute HOD in H_2O/salt solutions. The OD stretch is studied to eliminate vibrational excitation transfer, which interferes with the dynamical measurements. Though previous research suggested that only the anion affected dynamics in solution, here it is shown that the cation plays a role as well. From FT-IR spectra of the OD stretch, it is seen that replacing either ion of the salt pair causes a shift in absorption frequency relative to that of the OD stretch absorption in bulk pure water. This shift becomes pronounced with larger, more polarizable anions or smaller, high charge-density cations. The vibrational lifetime of the OD hydroxyl stretch in these solutions is a local property and is primarily dependent on the nature of the anion and whether the OD is hydrogen bonded to the anion or to the oxygen of another water molecule. However, the cation still has a small effect. Time dependent anisotropy measurements show that reorientation dynamics in these concentrated solutions is a highly concerted process. While the lifetime, a local probe, displays an ion-associated and a bulk-like component in concentrated solutions, the orientational relaxation does not have two subensemble dynamics, as demonstrated by the lack of a wavelength dependence. The orientational relaxation of the single ensemble is dependent on the identity of both the cation and anion. The 2D IR vibrational echo experiments measure spectral diffusion that is caused by structural evolution of the system. The vibrational echo measurements yield the frequency−frequency correlation function (FFCF). The results also show that the structural dynamics are dependent on the cation as well as the anion.

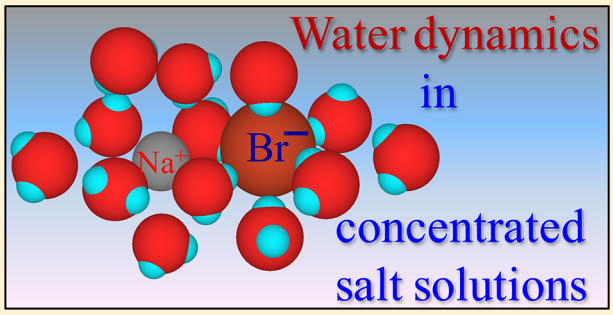

I. INTRODUCTION

Aqueous salt solutions are ubiquitous. They occur inside living cells, the ocean, and in many industrial chemical processes. The physical changes in structure and dynamics that ions exert on aqueous solutions are central to understanding and controlling processes. The ability of water to form up to four hydrogen bonds gives it unique liquid properties. Water hydrogen bonds are not static but continually break and reform in an extended network of concerted motions encompassing at least the first and second solvation shells.[1,2] When the water molecules interact with other species, they are unable to form hydrogen bonds in the same manner as bulk water. Water in a reverse micelle,[3−11] next to a solute ion,[12,13] mixed with another solvent,[14,15] in zeolite cavities,[16] in the channels of a polyelectrolyte fuel cell membrane,[3,17] or in an ionic liquid[18] has perturbed hydrogen bond networks that can cause a slowing in the dynamics of water, sometimes dramatically. Understanding the dynamics of water in complex environments is important for understanding many physical and biological processes, such as proton transport in fuel cell membranes and protein folding, but it is also challenging because the dynamics of the water structure occur on the hundreds of femtoseconds to picoseconds scale.[19,20] Thus, ultrafast mid-infrared spectroscopy is utilized to probe the dynamics of these systems. NMR has also been used to quantify water's dynamics and the B coefficients obtained for different salts are affected both by cations and anions but pertain only to dilute solutions.[21] Another study of more concentrated solutions found it difficult to separate individual ion values.[22]

While the ultrafast dynamics of water in ionic solutions have been studied by mid-IR ultrafast experiments to some extent,[12,13,23,24] these studies have focused mainly on the influence of the anion and explored mostly alkali-halide pairings. From these studies, it was found that the nature of the anion played a significant role in blue shifting the OD stretch spectrum of dilute HOD in H_2O and slowing the dynamics of the water, with the cation playing little, if any, role.[24−26] A recent study, however, suggested that $MgSO_4$ has a dramatic slowing effect on the aqueous orientational relaxation dynamics, which is unexplained by appealing solely to the contribution of the sulfate.[27] The authors concluded that the cation and anion effects on the solution's water dynamics are interdependent and nonadditive. Another study of highly concentrated salt solutions interpreted time dependent data on the influence of ions on water reorientation using two distinct subensembles of water molecules: water molecules interacting with ions and water molecules that behaved like bulk water.[28]

Received: September 25, 2012
Published: October 31, 2012

The study saw a dependence on the cation, provided the cation was sufficiently small.[28] Because of the very high concentration of ions in the solutions that were studied, the apparent presence of a bulk water component seems at odds with the current understanding of highly concentrated ionic solutions[29] and how reorientation slowing occurs, and necessitates a closer examination of salt solutions and the cation's influence on their dynamics.

Here we report the results from polarization selective IR pump−probe experiments as a function of wavelength and 2D IR vibrational echo experiments used to study a variety of aqueous salt solutions. The OD hydroxyl stretching mode of dilute HOD in H_2O is probed in the experiments. The OD stretch is studied to eliminate vibrational excitation transfer,[30−34] which can interfere with the dynamical measurements. Simulations of bulk water have shown that dilute HOD does not change water's dynamics and that the OD hydroxyl stretch reports on the dynamics of the overall water hydrogen bond network.[35] A variety of salt solutions with both monovalent and divalent cations and anions are investigated. FT-IR measurements of the OD absorption in the different salt solutions are also presented.

From the FT-IR spectra of the OD stretch, it is seen that replacing either ion of the salt pair causes a shift in absorption frequency to the red or to the blue relative to that of the OD stretch absorption in bulk pure water. This shift becomes pronounced with larger, more polarizable anions or smaller, high-charge-density cations. The vibrational lifetime of the OD hydroxyl stretch in these solutions is a local property and is primarily dependent on the nature of the anion and whether the OD is hydrogen bonded to the anion or to the oxygen of another water molecule. However, the cation still has a small effect. Time dependent anisotropy pump−probe measurements show that reorientation dynamics in these concentrated solutions is a highly concerted process. While the lifetime, a local probe, displays an ion-associated and a bulk-like component, the orientational relaxation does not have two subensemble dynamics, as demonstrated by the lack of a wavelength dependence. The orientational relaxation is dependent on the identity of the anion and the cation. However, instead of each affecting a separate subensemble, the solutions studied show the combination has an overall combined effect on the reorientation. The 2D IR vibrational echo experiments measure spectral diffusion that is caused by structural evolution of the system. Spectral diffusion is manifested by the time dependent change in shape of the 2D IR spectrum. This shape change is used to obtain the frequency−frequency correlation function (FFCF). The results show that the structural dynamics are dependent on the cation as well as the anion.

II. EXPERIMENTAL PROCEDURES

Salts were obtained from Sigma-Aldrich and were used as received without further purification. Water used in these experiments is a 5% HOD in H_2O solution, with the OD stretch functioning as a vibrational probe. Salt solutions were prepared by weight. Samples were assembled by sandwiching a portion of the solution between two CaF_2 windows separated by a Teflon spacer of sufficient thickness so the optical density of the sample peak absorption was between 0.3 and 0.5. Infrared spectra were taken with a Thermo Scientific Nicolet 6700 FT-IR spectrometer. The spectrum of an identical sample, but made with pure H_2O instead of 5% HOD, was subtracted from the sample spectrum to give the FT-IR of the OD stretch alone.

The output of a Ti:sapphire regenerative amplifier was converted by an optical parametric amplifier to the near-IR. This light was then difference-frequency-mixed in a $AgGaS_2$ crystal to create ∼4 μm, ∼70 fs mid-IR pulses. This light was then split into two beams for the pump−probe experiment or four beams for the vibrational echo. For the pump−probe experiments, the pump polarization was rotated 45° relative to the probe and chopped. The two beams crossed in the sample, and the components of the probe parallel and perpendicular to the pump were selected by a polarizer on a computer-controlled rotation mount. The probe pulse (signal) was dispersed by a monochromator acting as a spectrograph and detected on a 32 pixel, liquid nitrogen cooled, mercury−cadmium−telluride array detector. The experimental setup was purged with air scrubbed of water and carbon dioxide to minimize background absorption of the IR pulses.

For the vibrational echo experiments, three IR pulses impinged on the sample and stimulated the emission of the vibrational echo that propagates in a unique direction. The vibrational echo was then heterodyned with a fourth pulse. The time between the first two pulses is called τ, and the time between pulse 2 and 3 is called T_w. Data were collected by scanning τ at a fixed T_w, heterodyning the signal, and resolving the signal with the IR array detector after it passed through a monochromator used as a spectrograph.[36] The resulting interferograms were numerically Fourier transformed at each wavelength to give 2D spectra. At each T_w, the 2D spectra have different band shapes due to spectral diffusion, which reflects the amount of structural evolution that has taken place. Details on the experimental layout and procedures for 2D IR can be found elsewhere.[7,36]

III. RESULTS AND DISCUSSION

A. Absorption Spectra. The OD stretch is essentially a single local mode and thus gives rise to a fairly simple absorption spectrum.[37,38] The OD spectrum of HOD in H_2O is very broad due to varying strengths and different numbers of hydrogen bonds.[38−40] Subensembles of water with stronger and/or more hydrogen bonds absorb at redder wavelengths, and those with weaker and/or fewer are blue-shifted. The introduction of salt into a solution modifies the hydrogen bonding of pure water as the water molecules arrange to solvate the ions. OD hydroxyls that are bound to anions have a distinct environment from ODs bound to the oxygens of other water molecules. Even in a highly concentrated salt solution, some ODs will be bound to anions and some to other water molecules. The observed spectrum is the sum of the contributions of all species in solution, and thus can be decomposed into approximately Gaussian distributions resulting from the water−water and water−ion interactions. A greater observed shift in the spectrum will occur if either the number of affected waters increases (higher salt concentration) or the influence of the ions (both anions and cations) causes a larger shift.

Figure 1 displays FT-IR spectra at various concentrations of two of the salt solutions that were studied, NaBr (A) and $MgSO_4$ (B). Note that there are small anomalies in some of the spectra around 2350 cm^{-1} caused by incomplete purging of CO_2, which absorbs very strongly in this region. In the NaBr solutions, the OD spectrum shows a blue shift relative to the spectrum of HOD in pure H_2O. The blue shift becomes more

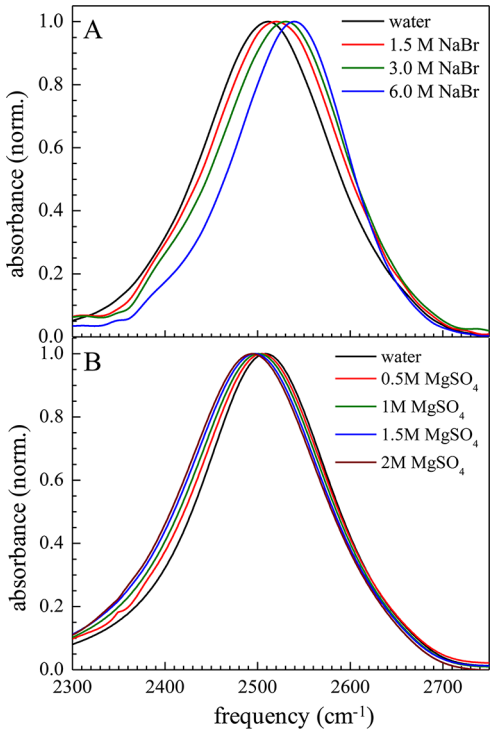

Figure 1. Background subtracted FT-IR of the OD stretch in NaBr and $MgSO_4$ aqueous solutions. Note that the NaBr experiences a blue shift with increasing salt concentration (A), while $MgSO_4$ undergoes a red shift (B).

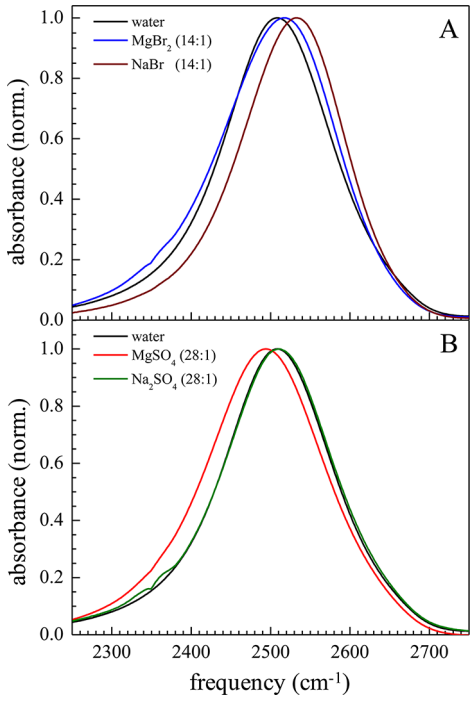

Figure 2. Background subtracted FT-IR of the OD stretch of solutions with the same anion and ratio of water to that anion. If the spectrum were dependent on the anion alone, these curves would be identical. The presence of magnesium rather than sodium causes a shift toward the red.

pronounced as the salt concentration increases (see Figure 1A). The blue shift is frequently interpreted as the water hydroxyl making a weaker hydrogen bond to the Br^- than it does to the oxygen of another water molecule. The spectrum is the sum of spectra of OD hydroxyls bound to Br^- and bound to oxygens of water. As the number of ODs interacting with Br^- ions increases (as the concentration is raised), the amplitude of the blue-shifted component of the spectrum increases relative to the component of hydroxyls bound to water oxygens that give rise to a bulk-like water spectrum. Therefore, increasing the concentration causes an increasing blue shift of the entire spectrum (see Figure 1A). As the size of the halide increases, e.g., Cl^-, Br^-, and I^-, the shift becomes more pronounced due to the decreased charge density of the anion causing the ion–hydroxyl interactions to become weaker.[26] Changing the monovalent cation seemed to have no effect on the absorption spectrum of the halide salts; thus, it was concluded that the anion was primarily responsible for the spectral shift.[41,42] This was seen to be the case with perchlorate salts as well.[43]

Magnesium sulfate, however, does not follow the same trend. $MgSO_4$ solutions show a red shift with increasing concentration (see Figure 1B). This would seem to indicate that sulfate interacts strongly with water. However, other sulfate salts do not show the same extent of a red shift. Moreover, not all bromide salts show the same extent of a blue shift, as seen with NaBr. These differences depend on the cation. Figure 2A shows the spectrum of the OD stretch in NaBr and $MgBr_2$ aqueous solutions and the spectrum of HOD in pure H_2O. For both salt samples, there are 14 water molecules per Br^-. Changing the cation from Na^+ to Mg^{2+} produces a spectrum that is not as blue-shifted, although the number of anions per water molecule is the same. Figure 2B shows the spectrum of the OD stretch in $MgSO_4$ and Na_2SO_4 aqueous solutions and the spectrum of HOD in pure H_2O. There are 28 water molecules per SO_4^{2-}, which is 14 water molecules per negative charge, the same as in the Br^- solutions of Figure 2A. The spectrum of the Na_2SO_4 solution is blue-shifted relative to the $MgSO_4$, although there is the same number of water molecules per anion. It is interesting to note that the OD spectrum in the sodium sulfate solution is virtually identical to that in pure water. In rubidium sulfate (not shown), the OD spectrum shows a very slight blue shift relative to OD in bulk water. These results show that the anion is not solely responsible for the spectral shift; the cation matters as well.

Why then was a dependence on cation not seen in the halide salts? The cations used in many experiments were larger monovalent ions. However, when magnesium is swapped for sodium as a counterion to bromide, the spectrum does change. Thus, the effect of the cation is not limited to sulfates but extends to the halides, provided the cation has a sufficiently high charge density, nor is the effect limited to magnesium. Spectra of the OD stretch in solutions of nickel and copper sulfates (not shown), in which the cations have approximately the same charge density as magnesium, show the same red shift as magnesium sulfate solutions. Using double difference spectroscopy, this effect has been documented in the literature[41,44] with cations of greater polarizing power shifting the linear spectrum of waters bound to them to the red. There seems to be a threshold, set by the anion, at which cation charge density is sufficient to observe this effect.

The experimentally observed spectra of salt solutions are made up of contributions from more than one population, and the spectra associated with these populations are offset (with the exception of Na_2SO_4). Therefore, at each wavelength, there is a different and well-defined contribution from each component. For example, the spectrum of the OD stretch in

dx.doi.org/10.1021/jp3095402 | J. Phys. Chem. B 2012, 116, 13781–13792

a KI solution, which is blue-shifted relative to HOD in pure H_2O, is shown in Figure 3A (black curve). This solution has 12

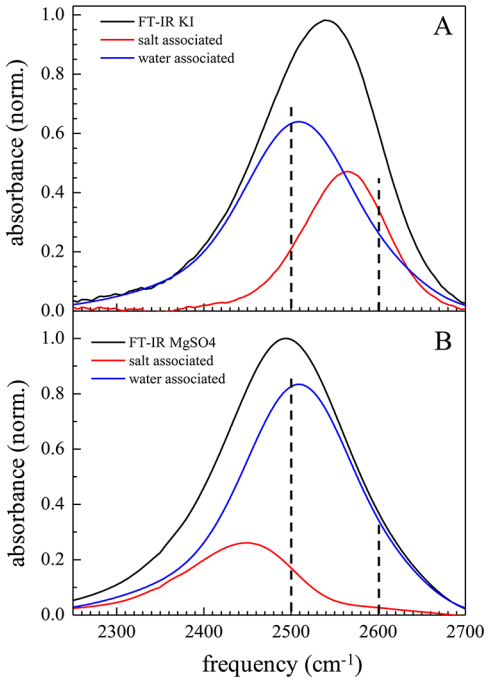

Figure 3. Illustration of the decomposition of 12:1 KI (A) and 28:1 $MgSO_4$ (B) spectra into distributions of water-associated and salt-associated hydroxyls (see text for method). Note that the percentage of water-associated water is different for each wavelength.

water molecules per ion pair. The blue curve is the absorption of ODs that are hydrogen bonded to the oxygen of a water molecule (water-associated). The red curve is the extracted spectrum of ODs interacting with I^- anions (salt-associated). The following procedure is used to separate the spectrum into a bulk-like OD/H_2O component and the salt-associated component. The spectrum of OD in pure H_2O is not Gaussian; it has a tail to the low frequency side. The central part of the OD/H_2O spectrum was fit to a Gaussian. The total FT-IR OD spectrum in salt solution (black curve in Figure 3A,B) was fit to two Gaussians, one with fixed peak position and width, which is the OD/H_2O Gaussian approximation, and the other is the salt-associated OD spectrum. Using the amplitude of the OD/H_2O spectrum from the fit, the actual OD/H_2O spectrum (red tail included) is subtracted from the experimental FT-IR spectrum to yield the salt-associated spectrum (red curve in Figure 3A,B). Though these fits are approximate, the ratio of the area under the curves corresponds to the percentage of hydroxyls that are expected to be in the first solvation shell of the anion; thus, the decomposition is reasonable. Moreover, once generated, the decomposition curves satisfactorily fit any concentration of the solution when the amplitudes are scaled to reflect the relative amount of each ensemble in solution. While this procedure will have some error, it provides a good approximation of the spectra of the two components, and it is sufficient for what follows.

The important point shown in Figure 3 is that the contribution from ODs associated with water oxygens and ODs that are bound to anions change with wavelength. At 2500 cm^{-1} (see Figure 3), 75% of the ODs in KI (Figure 3A) are associated with oxygens of water molecules, while at 2600 cm^{-1} the number drops to 43%. Note that at these same wavelengths the fractions for $MgSO_4$ (Figure 3B) are very different, since the salt causes an overall red shift instead of a blue shift. This weighting factor will be taken into account when comparing the time dependent responses at different wavelengths. For systems with spectra like those depicted in Figure 3, if water-associated and salt-associated ODs have different dynamics, then the measured dynamical curves will change with wavelength, since the ratio of two subensembles changes. If there is no wavelength dependence, then the two subensembles do not have dynamics that are distinct for the particular dynamical observable being measured.

B. Population Relaxation. The vibrational lifetimes are extracted from pump−probe data and report on how quickly vibrational energy leaves the excited OD stretching mode. This energy dissipates into the system into a combination of lower frequency modes, including bending, torsion, and bath modes that sum to the original energy.[45,46] The lifetimes can be obtained from polarized pump−probe experiments. The collected parallel and perpendicular components of the probe signal, $S_{\parallel}(t)$ and $S_{\perp}(t)$, can be expressed in terms of population relaxation, $P(t)$, and the orientational relaxation correlation function, which is the second Legendre polynomial correlation function, $C_2(t)$.

$$S_{\parallel} = P(t)[1 + 0.8C_2(t)] \quad (1)$$

$$S_{\perp} = P(t)[1 - 0.4C_2(t)] \quad (2)$$

Then, the normalized population relaxation is

$$P(t) = S_{\parallel}(t) + 2S_{\perp}(t) \quad (3)$$

In the experiments, vibrational relaxation deposits a small amount of heat into the sample, which produces constant isotropic signal at long time.[47] This heating offset is removed from $S_{\parallel}(t)$ and $S_{\perp}(t)$ using a procedure developed previously.[47]

$P(t)$ data are fit to a single or biexponential decay at each wavelength:

$$P(t) = Ae^{-t/\tau_1} + (1 - A)e^{-t/\tau_2} \quad (4)$$

where A is the amplitude and τ_1 and τ_2 are the vibrational lifetimes. If a single exponential is used, $A = 1$. The fit results are normalized, so A and $(1 - A)$ are the fractions of each component. In general, the vibrational lifetime of the OD stretch is sensitive to local environment, so the presence of a biexponential decay shows that there are two separate hydrogen bonding environments. One environment consists of OD bound to a water oxygen, and the other of OD interacting with the anion. The oxygen of HODs associated with cations do not have ODs directly hydrogen bonded to them, as the anions do, and so the perturbation of the vibrational relaxation is expected to be small compared to the direct effect of OD bound to anions. Previous studies have shown that ODs interacting with monovalent anions have a longer lifetime than OD in pure H_2O.[4,5,12,48] However, it is also possible (see below) that the anion-associated OD hydroxyl has the same or almost the same vibrational lifetime as the OD bound to a water oxygen. Therefore, it is possible to observe a single exponential $P(t)$ even though there are two environments.

Representative population relaxation curves for the OD stretch in the most concentrated salt solutions and the decay in pure water are shown in Figure 4A. The numbers in parentheses in the figure are the number of water molecules

dx.doi.org/10.1021/jp3095402 | J. Phys. Chem. B 2012, 116, 13781−13792

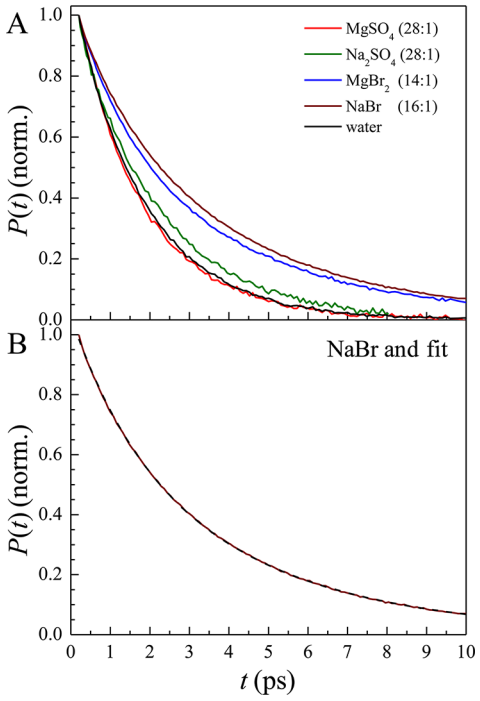

Figure 4. Population relaxation for comparable concentrations of salt solutions (A) at 2570 cm^{-1}. The $MgSO_4$ curve is nearly identical with that of water, while Na_2SO_4 is slightly slower. The bromide vibrational relaxations are much slower than the sulfates, and display a wavelength dependence (see Figure 7) suggesting two environments in solution. Thus, the bromide curves are fit to a biexponential decay, one of which is illustrated in part B.

per anion. All of the salt solutions have about the same number of water molecules per negative charge. The bromide population relaxations fit to biexponential decays, clearly demonstrating the presence of two distinct environments. For the biexponential fits, τ_1 is fixed to the value for bulk water, 1.7 ps,[4,5] and the other longer lifetime is allowed to float. Figure 4B shows an example of one of the fits. The data are from the NaBr solution (red curve) and the biexponential fit (the dashed black curve). The data and the fit are essentially indistinguishable. From this fit, the fraction of salt-associated water molecules ($1 - A$) is also determined as a function of wavelength. Results for all of the $P(t)$ fits are give in Table 1. For the bromide solutions, the identity of the cation has a negligible effect on the population relaxation.

The sulfate solutions show population relaxation that can be fit very well as a single exponential (see Figure 5A). The resulting lifetime is not significantly different from bulk water. The appearance of only one decay constant does not necessarily signify that there is only one hydrogen bonding environment but could mean that the vibrational lifetimes of OD in the solution's different environments are not sufficiently dissimilar to be distinguishable. The OD vibrational lifetime in $MgSO_4$ solution has a decay constant that is 1.7 ps, which is identical to that of bulk water. There is no dependence on concentration. However, the Na_2SO_4 and Rb_2SO_4 solutions give an indication that all of these sulfate solutions have two environments associated with vibrational relaxation in the same manner as NaBr. Figure 5A shows a single exponential fit (red, dashed curve) to the vibrational relaxation data (green, solid curve) for the Na_2SO_4 28:1 solution. The decay constant is 2.1 ps. Figure 5B shows a biexponential fit to the same data. One

Table 1. Population Relaxation Parameters for Several Salt Solutions and Water

salt	water:anion	A	τ_1 (ps)	τ_2 (ps)
NaBr[a]	16:1	0.41 ± 0.05	1.7	4.4 ± 0.2
$MgBr_2$[a]	14:1	0.37 ± 0.05	1.7	4.6 ± 0.2
	28:1	0.72 ± 0.05		4.4 ± 0.2
$MgSO_4$	28:1, 37:1, 56:1, 113:1	1	1.7 ± 0.1	
Na_2SO_4	28:1	1	2.1 ± 0.1	
	56:1		1.8 ± 0.1	
$NiSO_4$	28:1	1	1.6 ± 0.1	
$CuSO_4$	41:1	1	1.7 ± 0.1	
Rb_2SO_4	28:1	1	2.1 ± 0.1	
	56:1		1.8 ± 0.1	
water[3]		1	1.7 ± 0.1	

[a]Fractions are for 2570 cm^{-1} (see spectrum, Figure 2A). The fraction increases for redder wavelengths.

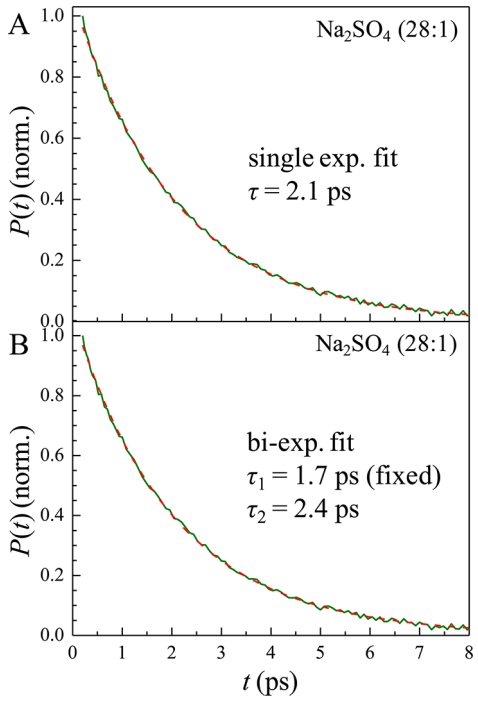

Figure 5. Two fits of the population relaxation of the 28:1 Na_2SO_4 solution. Note that this curve can be fit to either a single exponential yielding a lifetime slightly longer than that of bulk water or to a biexponential. This suggests that there are two lifetimes from the two environments in solution (water-associated or salt-associated) but that they are very similar and thus hard to distinguish.

decay constant (τ_1) is fixed at 1.7 ps, the vibrational lifetime of OD in bulk water.[4,5] The other decay constant is allowed to float and yields τ_2 = 2.4 ps. The point is that the apparent single exponential decay can be composed of two decays with almost the same time constant. When the Na_2SO_4 concentration is reduced to 56:1, the single exponential fit time constant becomes faster (1.8 ps) as would be expected for two ensembles, as the fraction that is anion-associated (slower component) contributes a smaller amplitude to the decay.

The $MgSO_4$ solutions do not show a concentration dependence because, by serendipity, the relaxation of the anion-associated ODs has a virtually identical lifetime as ODs bound to water oxygens. This uniform decay of 1.7 ps extends

dx.doi.org/10.1021/jp3095402 | J. Phys. Chem. B 2012, 116, 13781−13792

across the line width from the very blue wavelengths that are entirely water−water interactions to the far red which should be primarily salt-associated waters, according to the FT-IR decomposition (see Figure 3B). The dynamics of the red side of the line were accessed by looking at the red side of the 1 to 2 transition,[47] since the red side of the 0 to 1 is obscured by overlap with the blue side of the 1 to 2.

For the sulfate salts, divalent cation solutions (Mg^{2+}, Ni^{2+}, and Cu^{2+}) display single exponential decay constants faster than those from monovalent cation solutions (Na^+, Rb^+). This difference demonstrates that the cation has a small but measurable influence on the vibrational lifetime.

C. Orientational Relaxation. Orientational relaxation parameters are obtained from the pump−probe data by calculating the polarization anisotropy, $r(t)$, from the difference between the parallel and perpendicular signals.

$$r(t) = \frac{S_{\parallel}(t) - S_{\perp}(t)}{S_{\parallel}(t) + 2S_{\perp}(t)} = 0.4C_2(t) \tag{5}$$

The term in the denominator removes the population relaxation (see eq 3 and below).

The vibrational lifetime limits the experimental time window over which the anisotropy can be collected; thus, the anisotropy cannot be observed decaying all the way to zero, which introduces some uncertainty in the fitting. Anisotropy curves for selected concentrated solutions appear in Figure 6. Note

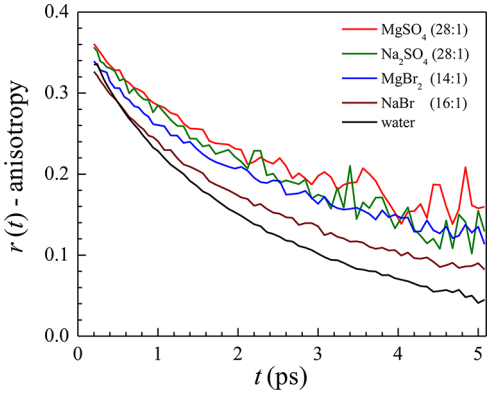

Figure 6. Anisotropy decay curves for comparable concentrations of salt solutions, recorded somewhat blue of the line centers. Note that NaBr has a much faster decay than $MgBr_2$, suggesting that the cation can play a large role in orientational relaxation. $MgSO_4$ and Na_2SO_4 do not show such a dramatic difference.

that the anisotropy decays do not start from 0.4 as the above equation suggests. This is due to an ultrafast inertial component that occurs on the tens of femtoseconds time scale and is obscured by the very large nonresonant signal from the sample.[49] The amplitude of this inertial component can be determined from the difference between 0.4 and the $t = 0$ anisotropy determined by extrapolating the experimental curves the short distance from 200 fs back to 0. This inertial component varies with wavelength, as has been documented in the literature.[50] The variation is small for the blue wavelengths examined but becomes more pronounced for wavelengths on the red side of the 1 to 2 transition, which shows the same dynamics as the red side of the 0 to 1 transition. In the following, only the anisotropy decays after the inertial component are discussed.

Within experimental error, the anisotropy decay of pure water is a single exponential with a time constant of 2.6 ps.[51] If solvating an ion leads to two distinct types of water, water interacting with ions and bulk-like water, which have different rotation times, the anisotropy decay will not be a single exponential. Such nonexponential anisotropy decays are seen in large reverse micelles where there is water at the interface, which undergoes slow orientational relaxation, as well as bulk-like water at the core (reverse micelle center region) which can rotate more freely with bulk water anisotropy decay.[4,52]

If there are two distinct subensembles of water molecules which have different vibrational lifetimes as well as different anisotropy decays, the contribution to the anisotropy of the different rates of reorientation are weighted by the lifetimes and give rise to the two-component model.[4] The anisotropy at a given wavelength is described by

$$r(t) = r_0\left[\frac{Ae^{-t/\tau_1}e^{-t/T_{or1}} + (1-A)e^{-t/\tau_2}e^{-t/T_{or2}}}{Ae^{-t/\tau_1} + (1-A)e^{-t/\tau_1}}\right] \tag{6}$$

where A is the amplitude and τ_1 and τ_2 are the vibrational lifetimes from the fit of the population relaxation, T_{or1} and T_{or2} are the reorientation times of the two populations, and r_0 is an adjustable parameter corresponding to the value of the anisotropy following the initial drop from 0.4 caused by the ultrafast inertial component. The value of r_0 can be read off the data within a small margin of error. Equation 6 can produce a variety of nonexponential curves. Depending on the parameters, the decays can be monotonically decreasing, decay to a plateau and then decay further, or decay, increase, and then finally decay to zero.[4,53] As the amplitude of the two components changes with wavelength, the shapes of the decay curves will vary substantially.

If the lifetimes are the same or almost identical, eq 6 reduces to a biexponential decay of the anisotropy given by

$$r(t) = r_0[ae^{-t/T_{or1}} + (1-a)e^{-t/T_{or2}}] \tag{7}$$

where a is the fraction associated with T_{or1}. The factor a has to be determined from the fit of the anisotropy, since it cannot be derived from the fit of the population relaxation (as was the case with A above) if the lifetimes are indistinguishable. If there are two subensembles with different orientational relaxation times, then the anisotropy will vary with wavelength, since the fraction, A (or a), of the two populations is wavelength dependent. It is important to note that the anisotropy decay can be biexponential for reasons other than having two subensembles with different orientational relaxation times and the same lifetimes. As discussed below, the wobbling-in-a-cone model[5,49,54] produces a biexponential decay. The wavelength dependence of the anisotropy decay is the key to sorting out the nature of the orientational relaxation.

The FT-IR spectra of bromide solutions show a blue shift from bulk water. As an example, we will consider the $MgBr_2$ system. The FT-IR spectrum of $MgBr_2$ and its decomposition into ion-associated hydroxyls and water-oxygen-associated hydroxyls is similar to that shown for KI in Figure 3A. There are more ion-associated hydroxyls to the blue and more water-associated hydroxyls to the red. Thus, at each wavelength, there is a different ratio of the two components. The water-associated hydroxyls and the ion-associated hydroxyls have lifetimes of 1.7 and 4.5 ps, respectively (see Table 1). Figure 7 shows population relaxation data for the $MgBr_2$ solution (14:1) at several wavelengths over which the ratio of the two

dx.doi.org/10.1021/jp3095402 | J. Phys. Chem. B 2012, 116, 13781−13792

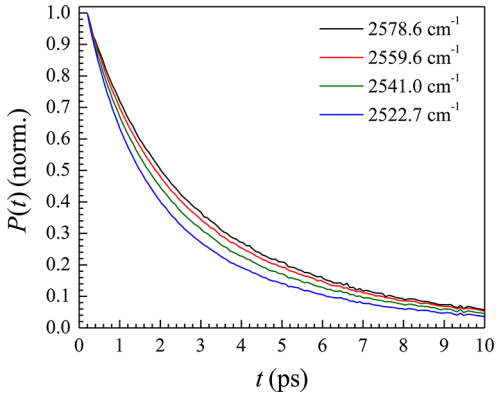

Figure 7. Population decay, $P(t)$, for the 28:1 $MgBr_2$ solution at different detection wavelengths. Note that the decay slows as the detection wavelength is shifted to the blue. This is due to the fraction of salt-associated hydroxyls increasing, thus slowing the population relaxation at these wavelengths. This trend is typical for having two populations with different dynamics.

components change. As can be seen in the figure, the population decay curves are wavelength dependent. At each wavelength, the two decay constants are the same, but the amplitude factor, A (see eq 4), varies. Both the spectrum and the lifetime are determined by the immediate environment of the hydroxyl (water-associated or ion-associated), giving two components to the spectrum and two components to the population relaxation.

As discussed above, orientational relaxation is a concerted process that involves at least the first and second solvation shells of a given water molecule,[1,2] an HOD in the experiments presented here. Therefore, the very local interactions of a hydroxyl are insufficient to completely determine the orientational relaxation, since they do not take into account the dynamics of the neighboring water molecules. Figure 8A shows HOD anisotropy decays in the same $MgBr_2$ solution used for Figure 7. Ten wavelengths are shown. There is no wavelength dependence. Note that the noise in the different curves is the same because all the wavelengths were taken simultaneously using the array detector. Laser amplitude fluctuations will therefore affect all wavelengths in the same manner. If the solution contained regions of bulk-like water and water−ion regions,[27,28] then there would be a wavelength dependence. If these two types of populations did in fact exist, they would have their own unique reorientation dynamics. Changing the ratio of the components by changing the wavelength would cause the anisotropy to vary with wavelength just as the population relaxation shown in Figure 7 does. Figure 8B shows the orientational relaxation of the OD stretch of HOD in water in large AOT reverse micelles as a function of wavelength. The data are taken from the literature.[4] In the reverse micelle, there are two ensembles that are spatially distinct. There is bulk-like water in the core of the reverse micelle (region well removed from the interface), and there is water associated with the sulfonate anionic head groups at the water−surfactant interface. The two subensembles have different lifetimes and different orientational relaxation rates. The anisotropy decays display substantial wavelength dependence. The lines through the data are fits using eq 6.[4]

What is remarkable about Figure 8A is that there is no distinction between the orientational relaxation dynamics for OD hydroxyls that are ion-associated or water-associated.

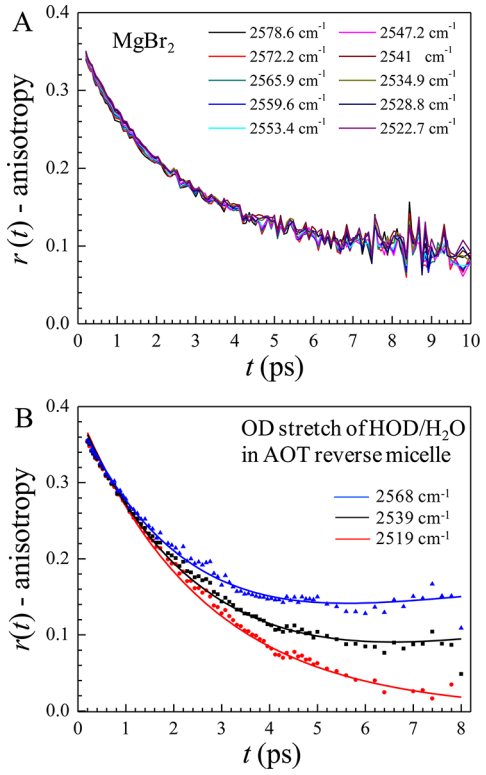

Figure 8. Anisotropy, $r(t)$, for the 28:1 $MgBr_2$ solution at different detection wavelengths (A). Note that the decay does not vary appreciably with wavelength. The noise is correlated because the wavelengths are all collected at the same time on the array detector. Compare this with the wavelength dependent anisotropy of a large AOT reverse micelle (B), reproduced from the literature,[4] which does show two distinct populations: bulk and interfacial water.

Orientational relaxation involves many water molecules. Reorientation of water requires the concerted rearrangement of many hydrogen bonds in a process referred to as jump reorientation.[1,2] No single water molecule can undergo reorientation without many other water molecules also undergoing reorientation. In a concentrated salt solution, reorientation of any water molecules will be influenced by the presence of the ions. There are no regions of water that are sufficiently large to produce a component of the orientational relaxation that has the bulk water reorientation time of 2.6 ps. In dilute salt solutions, there will be regions that are so far from an ion that water will behave like bulk water, but this is not the case in concentrated solutions, which is in contrast to suggestions that have been made in some publications.[27,28]

Figure 9 shows the FT-IR spectrum of the OD stretch in a solution of $MgSO_4$ (28:1) and its decomposition into ion-associated and water-associated. It is important to emphasize that for our purposes it is not necessary for the decomposition to be exact. The spectrum is used to determine the spectral regions in which the OD will be ion-associated or water-associated. The overall spectrum is red-shifted relative to bulk water because the ion-associated OD hydroxyls are substantially red-shifted. In the region labeled 1 (blue side of the line), the ODs are mainly water-associated. In the region labeled 2 (red side of the line), the ODs have a substantial ion-associated contribution. If being water-associated versus ion-associated affects the orientational relaxation time, there should be a substantial difference in the anisotropy decays in these two

dx.doi.org/10.1021/jp3095402 | J. Phys. Chem. B 2012, 116, 13781−13792

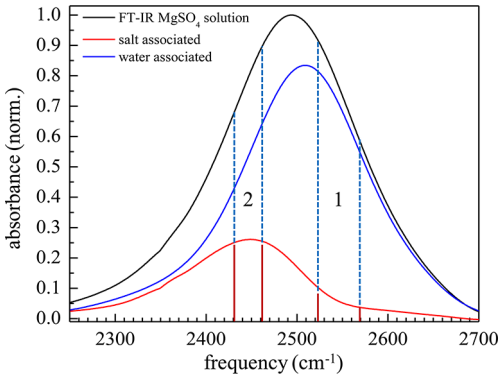

Figure 9. Decomposition of the FT-IR of the 28:1 $MgSO_4$ spectrum. Note that the wavelengths of interest (those that have a significant proportion of salt-associated water) occur on the red side of the spectrum and thus will be obscured by interference of the blue side of the 1 to 2. These wavelengths will be accessed by looking at dynamics on the red side of the 1 to 2, which correspond to the dynamics of region 2, just shifted by the anharmonicity to the red.

spectral regions. Experiments can be conducted in region 1. However, the anharmonicity of the OD stretch is ~140 cm^{-1}. Therefore, the peak of the 1−2 vibrational transition is at ~2355 cm^{-1}. The shape of the 1−2 band is very similar to the 0−1 band. In a pump−probe experiment, the 0−1 transition makes a positive signal, while the 1−2 transition makes a negative signal. In the region labeled 2, there is substantial overlap between the positive going 0−1 band (red side of the line) and the negative going 1−2 band. The overlapping portion of the 1−2 band is not only negative, but it also corresponds to the blue side of the line; that is, it will involve molecules that are on the blue side of the 0−1 band.

To obtain data corresponding to region 2 in Figure 9, experiments were conducted with the probe wavelength on the red side of the 1−2 transition between the wavelengths 2252 and 2327 cm^{-1}, which in terms of the molecules probed corresponds to region 2 in Figure 9. Figure 10 shows wavelength dependent anisotropy decay data for the $MgSO_4$ solution. The decays are identical within experimental error.

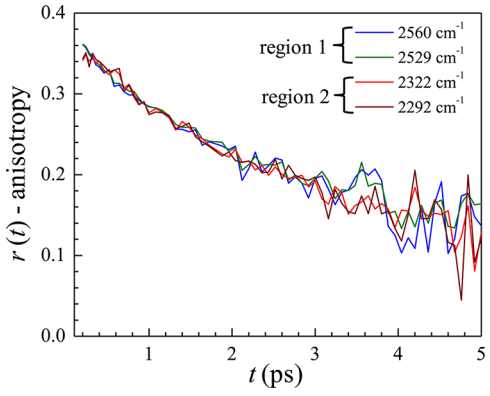

Figure 10. Comparison of the anisotropy from the red side of the 1 to 2 and the blue side of the 0 to 1 for 28:1 $MgSO_4$. The red wavelengths have been translated up by 0.025, since they experience a greater amount of motional narrowing than the bluer wavelengths. Other than this inertial drop, the anisotropy is the same across the line. This indicates a highly concerted reorientation process from a single ensemble and contradicts the theory that water-associated and salt-associated water reorient at different rates.

This is in spite of the fact that region 1 (see Figure 9) is overwhelmingly composed of water-associated OD hydroxyls and region 2 is composed of approximately 50−50 ion-associated and water-associated hydroxyls. Because of the large difference in the nature of the populations of regions 1 and 2, these anisotropy decays are a clear demonstration that there are not two distinct orientational relaxation populations that have two orientational relaxation times. The entire collection of water molecules undergoes orientational relaxation with the same dynamics, although some of the OD hydroxyls being probed are bound to sulfate anions and some are bound to the oxygens of other water molecules.

The lack of a wavelength dependence that spans the wavelengths in regions 1 and 2 of Figure 9 demonstrates that there are not two separate populations, bulk-like water and ion-perturbed water, giving rise to two distinct reorientation times. Therefore, it does not make sense to fit the anisotropy to a biexponential with two reorientation times, one of which is fixed at the bulk water value of 2.6 ps, as has been done previously.[27,28] Fitting to a two-subensemble model is an appropriate procedure when there is a substantial amount of water in each subensemble, and the subensembles are physically segregated into different areas. As mentioned above, a system with two such subensembles are large reverse micelles that have a defined core and interfacial regions which reorient separately (see Figure 8B). However, in concentrated salt solutions, there is not a sufficient amount of water for there to be two such separated subensembles.[29] Though a particular water molecule may not be directly bound to an ion, its reorientation will be constrained by neighboring waters that are. Since reorientation of water molecules occurs by concerted jump reorientation rather than continuous diffusion,[1,2] the availability of neighboring water molecules to participate in reorientation is critical. It has been demonstrated that jump reorientation also occurs for water molecules bound to anions.[55] The lack of wavelength dependence shows that reorientation in these solutions is a concerted process involving waters that are ion-associated and water-associated.

Although the anisotropy decays do not show a wavelength dependence, which demonstrates that there are not two distinct subensembles with different reorientation times, the decays are not single exponentials. Thus, the curves were fit to eq 7. Since the biexponential decays cannot be attributed to two populations giving rise to different reorientation times, we attribute the slower component to concerted jump diffusion and the faster, in accordance with previous studies,[9,12,17,28,54] to a local, restricted, diffusive motion called wobbling-in-a-cone.[54,56] Wobbling takes place on a time scale short compared to the rearrangement of hydrogen bond structure (through the breaking and reforming of hydrogen bonds) during which the OD can sample a restricted range of orientations but cannot completely randomize. The orientational correlation function is

$$C_2(t) = [S^2 + (1 - S^2)e^{(-t/\tau_w)}]e^{(-t/\tau_l)} \quad (8)$$

where S is the generalized order parameter that describes the degree of restriction, τ_w is the time constant for the wobbling motion, and τ_l is the time constant for the complete longer time scale orientational relaxation. In the biexponential fit, the longer time constant, T_{or2}, is equal to τ_l and $\tau_w = ({T_{or1}}^{-1} - {T_{or2}}^{-1})^{-1}$. Data for selected salts appear in Table 2. The cone angle is obtained from the order parameter using

$$S = 0.5 \cos\theta(1 + \cos\theta) \quad (9)$$

dx.doi.org/10.1021/jp3095402 | J. Phys. Chem. B 2012, 116, 13781−13792

Table 2. Orientational Relaxation Parameters for Several Salt Solutions and Water

salt	water:salt	fraction T_{or1}	T_{or1} (ps)	T_{or2} (τ_l) (ps)	τ_w (ps)	Θ (deg)
bulk water[3]		1	2.6			
$MgSO_4$	28:1	0.24 ± 0.03	0.9 ± 0.1	6.7 ± 0.4	1.0 ± 0.1	26 ± 1
	37:1	0.27 ± 0.03	1.0 ± 0.2	6.0 ± 0.4	1.2 ± 0.1	27 ± 1
	56:1[a]	0.32 ± 0.05	1.3 ± 0.2	4.9 ± 0.4	1.8 ± 0.2	31 ± 2
Na_2SO_4	28:1	0.31 ± 0.04	1.3 ± 0.3	6.4 ± 0.5	1.7 ± 0.2	30 ± 2
$MgBr_2$	28:1	0.34 ± 0.03	1.1 ± 0.2	7.1 ± 1	1.3 ± 0.2	32 ± 2
	56:1[a]	0.33 ± 0.03	1.0 ± 0.2	4.9 ± 0.3	1.3 ± 0.1	32 ± 3
NaBr	16:1	0.36 ± 0.04	1.2 ± 0.2	4.8 ± 0.4	1.6 ± 0.3	34 ± 3

[a]At these concentrations, there may be a bulk water component starting to grow in, but it cannot be distinguished from the salt due to low signal strength.

Using this formula, it was found that the cone angle in the most concentrated $MgSO_4$ solution was 26 ± 1°. This represents a similar level of restriction to the smallest AOT reverse micelles (29°)[3] and Nafion fuel cell membranes with low hydration levels (31 ± 2°).[17] This resemblance lends credence to the idea that salt in solution can influence water molecules much as an interface does, slowing the orientational relaxation dynamics. As the concentration of salt is decreased, the observed cone angle increases. This increase may be due to a lessening of the restriction placed on water molecules by the ions because of the introduction of more water molecules. It is also possible that, as more water is added, there begin to be separate populations in solution with different orientational relaxation times. Since the amplitude associated with such a separate population is small (and thus the amount of wavelength dependence it would add is also small enough to be within error), this motion cannot be distinguished from the wobbling and complete randomization. However, the presence of trace amounts of slower reorientation would show up in this analysis as a longer time constant for wobbling and an apparent increase cone angle, as is observed.

The cone angle for concentrated magnesium sulfate shows slightly more restriction than is found in sodium sulfate solutions, where the cone angle is 30 ± 2°. This hints at the effect of changing the cation but is not conclusive. NaBr solutions exhibit slightly less restricted motions than either of the sulfates, with a wobbling angle of 34 ± 3°. $MgBr_2$ solutions show similar behavior to the NaBr solutions, with a wobbling angle of 32 ± 2°. These wobbling angles represent a fair amount of restriction, as angles of 42 ± 3° have been seen both in midsized reverse micelles and in hydrated Nafion membranes.[3,17] The jump angle for reorientation of bulk water is 60°,[1] and it is similar in ionic solutions,[55] so these angles are firmly on the scale of wobbling rather than jump reorientation. However, even though the wobbling angles are essentially the same, the reorientation in $MgBr_2$ solutions is much slower than in NaBr. Therefore, the bromide is not the sole factor affecting the dynamics; changing the cation affects the dynamics.

Regardless of ion identity, as the concentration of salt increases, the anisotropy decay slows. Thus, more ions in solution lead to a greater restriction of water dynamics and causes the time for total reorientation to increase. The extent of this slowing is dependent on the identity of both the cation and anion.

D. 2D IR Vibrational Echo Spectroscopy. 2D IR vibrational echo experiments monitor structural dynamics through the time evolution of the 2D IR spectra of the OD hydroxyl stretch, which reports on spectral diffusion.[57,58] Spectral diffusion is quantified by the center line slope (CLS) method, from which the frequency−frequency correlation function (FFCF) is obtained.[36,59,60] The FFCF is the joint probability that a vibrational oscillator with a particular frequency at $t = 0$ will still have the same frequency at a later time t averaged over all initial frequencies. The decay of the FFCF is caused by structural changes in the system and is used to determine different time scales of structural evolution.

Simultaneous fitting of the CLS and the linear absorption spectrum provide the parameters for the FFCF. It should be noted that the relationship between the CLS and the FFCF was developed under the assumption of Gaussian fluctuations.[59,60] In systems such as bulk water, non-Condon effects and deviations from Gaussian fluctuations may influence experimental spectral observables to some extent.[61,62] Non-Condon effects account for a varying transition dipole with absorption frequency.[61,62] MD simulations have shown that the variations in calculated observables obtained via different water models are just as large as simulations that do or do not use the Gaussian approximation.[57,58,62,63] While obtaining the FFCF via the CLS method involves certain approximations, the CLS is still an easily accessible experimental observable that can discern time scales of structural fluctuations and can be used to compare different systems. Furthermore, the CLS is a valid observable that can be the target of simulations regardless of whether it is used to determine the FFCF.

The FFCF has frequently be modeled as a sum of exponentials

$$\mathrm{FFCF}(t) = \sum_{i=1}^{n} \Delta_i^2 e^{-t/\tau_i} \tag{10}$$

where Δ_i are the amplitudes and τ_i the correlation times of the frequency fluctuations induced by the structural fluctuation of the solution. In the motionally narrowed limit, $\Delta \cdot \tau < 1$ and Δ and τ cannot be determined independently but contribute to the homogeneous dephasing which is given as the total homogeneous line width. The homogeneous line width also has contributions from the vibrational lifetime and the orientational relaxation. However, in these systems, the pure dephasing contribution arising from ultrafast structural fluctuations overwhelms the other two contributions.

CLS curves for the OD stretch of HOD in selected concentrated salt solutions as well as pure water are shown in Figure 11. The numbers in parentheses in the figure's legend are the number of water molecules per salt "molecule". Because of the experimental time window set by the vibrational lifetime of the OD stretch, it is not possible to follow the decays all the way to zero. Table 3 gives the FFCF parameters for several

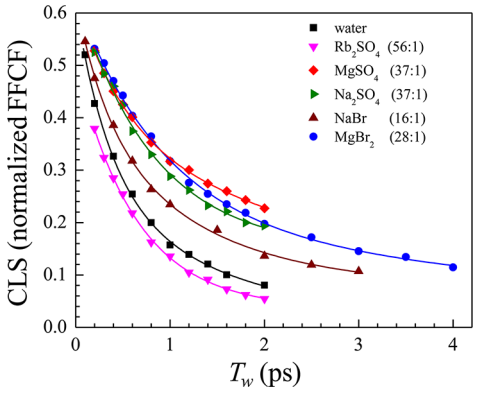

Figure 11. CLS curves for different salt solutions. Note that while $MgSO_4$ and Na_2SO_4 have similar decays, Rb_2SO_4 has a much faster decay. Also note the difference between NaBr and $MgBr_2$. These differences suggest that the identity of that cation does significantly affect the dynamics in solution.

solutions including some that are not shown in the figure. All of the solutions are fit with a three-component FFCF: a homogeneous component given as the homogeneous line width Γ and two components that describe the spectral diffusion. For bulk water (black square in Figure 11 and FFCF parameters in the first line of Table 3), simulations show that the short time scale dynamics arise from very local structural fluctuations of the hydrogen bond, mainly length fluctuations, while the slowest component reflects the complete structural randomization of the hydrogen bond network.[57,58]

In Figure 11, the data for water and Rb_2SO_4 56:1 (pink triangles) are virtually identical with the exception that the rubidium sulfate has a larger homogeneous component, as shown by the larger offset of the data from 1 at $T_w = 0$. The FFCF parameters for rubidium sulfate are given in the second line of Table 3. Within experimental error, the FFCF parameters for these two liquids are identical except for the larger homogeneous component of the rubidium salt solution. The vibrational echo experiment measures the dynamics of ODs in the entire solution, ion-associated and water-associated. At this low concentration, at least on the longest time scale associated with complete structural randomization of the liquid, there is little detectable difference between water and the rubidium sulfate solution.

The third line of Table 3 gives the FFCF parameters for $MgSO_4$ also at 56:1 concentration. In this solution, the slowest component of the FFCF is slightly slower than that for bulk water or the rubidium salt solution, although the error bars almost overlap. The Rb^+ cation is singly charged, and it is very large with an ionic radius of ∼1.7 Å.[64] In contrast, the Mg^{2+} cation is doubly charged and is small, with an ionic radius of ∼0.8 Å.[64] Therefore, the charge density on Mg^{2+} is much greater than that of Rb^+. This may be an indication that the charge density on the cation influences structural dynamics even at quite low concentration.

The fourth line of Table 3 (red diamonds in Figure 11) are the parameters for $MgSO_4$ at 37:1. Compared to the 56:1 solution, the slowest component of the FFCF (τ_2) has slowed substantially (and the faster component (τ_1) is also somewhat slower), but the error bars overlap to some extent. Thus, magnesium sulfate has some influence on the overall water dynamics at 56:1 concentration that increases substantially by 37:1. Line 5 of Table 3 gives the FFCF parameters for Na_2SO_4 solution. As seen in Table 3, at the 37:1 concentration with the sulfate anion, switching the cation from Mg^{2+} (Figure 11, red diamonds) to Na^+ (green triangles) does not change the dynamics within experimental error. Na^+ has an ionic radius of ∼1.15 Å,[64] which is significantly smaller than rubidium but substantially larger than Mg^{2+}. At this concentration and in the presence of the sulfate anion, changing the cation does not have much effect. However, for a monovalent anion, Br^-, the cation does make a significant difference. The CLS for NaBr (brown triangles) and $MgBr_2$ (blue circles) are shown in Figure 11, and the FFCF parameters are given in the last two lines of Table 3. The NaBr concentration is 16:1, while the $MgBr_2$ concentration is 28:1. However, the Br^- concentration in the $MgBr_2$ solution is 14:1, almost the same bromine anion concentration as in the sodium bromide solution. The Mg^{2+} cation causes substantially slower dynamics in solution than the Na^+ cation. The concentration of negative charges in these two solutions is only somewhat greater than the concentration of negative charges in the 37:1 sulfate solutions. Nonetheless, the cation appears to matter when the anion is singly changed but not when it is doubly charged. The results suggest that there is a threshold set by the anion at which the cation affects the salt solution dynamics.

It is important to recognize that the orientational relaxation correlation function (the second Legendre polynomial correlation function) obtained from the pump−probe experiments (Table 2) is a different correlation function than the FFCF (Table 3). Therefore, the resulting time constants cannot be directly compared. To make this point clear, for Gaussian diffusion orientational relaxation that is single exponential, dielectric relaxation, which measures the first Legendre polynomial correlation function, would give a time constant that is 3 times as long as a pump−probe experiment on the same system. Thus, the numbers obtained from pump−probe orientational relaxation and FFCF measurements are distinct.

Table 3. FFCF Parameters for Several Salt Solutions and Water

salt	water:salt	Γ	Δ_1	τ_1	Δ_2	τ_2
water[a]		76 ± 14	41 ± 8	0.4 ± 0.1	34 ± 11	1.7 ± 0.5
Rb_2SO_4	56:1	108 ± 7	42 ± 5	0.45 ± 0.1	30 ± 9	1.7 ± 0.5
$MgSO_4$	56:1	98 ± 3	38 ± 5	0.44 ± 0.1	42 ± 5	2.7 ± 0.5
$MgSO_4$	37:1	90 ± 2	39 ± 5	0.6 ± 0.1	45 ± 4	4.5 ± 1.0
Na_2SO_4	37:1	82 ± 6	42 ± 4	0.6 ± 0.2	39 ± 4	4.0 ± 0.6
NaBr[a]	16:1	74 ± 6	41 ± 3	0.5 ± 0.1	34 ± 4	3.5 ± 0.5
$MgBr_2$	28(14):1	93 ± 3	46 ± 4	1.0 ± 0.1	30 ± 6	8 ± 3.0

[a]Values reproduced from the literature.[12]

dx.doi.org/10.1021/jp3095402 | J. Phys. Chem. B 2012, 116, 13781−13792

IV. CONCLUDING REMARKS

FT-IR spectra, pump−probe spectroscopy, and 2D IR vibrational echo experiments were conducted to investigate the influence of ions in concentrated salt solutions on the dynamics of water. In the experiments, the OD stretch of dilute HOD in salt/H_2O solutions was used to investigate the properties of the solutions at high salt concentration. The results show that both the absorption spectra and the vibrational lifetimes are principally determined very locally by the immediate interaction of the OD hydroxyl with its hydrogen bonding partner, and thus by whether the hydroxyl is ion-associated or water-associated (hydrogen bonded to the oxygen of another water molecule). Absorption spectra can be decomposed into ion-associated and water-associated components (see Figures 1, 2, and 3). In general, the population relaxation is biexponential with one component having a decay time constant the same as that found for the OD stretch of HOD in pure H_2O and the other having a slower decay constant that depends mainly but not exclusively on the anion (see Figures 7 and 9 as well as Figures 4 and 5). For the absorption spectra and the population relaxation observables, it makes sense to divide the systems into two subensembles, ion-associated and water-associated. This division has also been seen very clearly in studies of reverse micelles with ionic surfactants.[4−6]

However, the detailed studies of orientational relaxation in the concentrated salt solutions demonstrate that a division of the orientational relaxation in two distinct subensembles, one with the bulk water orientational relaxation time and one with a slower relaxation time for the ion-associated water is not appropriate. In the concentrated solutions, the lack of a wavelength dependence for the orientational anisotropy decay reflects the fact that the reorientation is a concerted process,[1,2] and the orientational relaxation of any water, whether it is ion-associated or water-associated, depends on the hydrogen bond rearrangement of many surrounding water molecules. As shown in Figures 8 and 10, when the detection wavelength is moved so that the fractions of water molecules in the spectrum that are ion-associated and water-associated change substantially, there is no change in the orientational relaxation. The decay data curves fall right on top of each other within a small experimental uncertainty. Because water reorientation is a concerted process described as jump reorientation,[1,2] it involves many water molecules. In a concentrated salt solution, there are not regions of bulk-like water that can undergo bulk water reorientation, and regions of water in proximity of ions, which would have distinct reorientation dynamics. For reorientation in concentrated salt solutions, the system should be considered a single ensemble.

Of course, in dilute salt solutions, there will be two subensembles. At very low ion concentration, there will be large numbers of water molecules that are so far from an ion that they behave as if they are in pure water. There will also be some water molecules that are very close to an ion that will behave differently. At such high dilution, the types of IR experiments presented here cannot observe the ion-associated water molecules because all observables are overwhelmed by the contributions from the vast amount of bulk-like water. This type of division can be observed in large reverse micelles and lamellar structures.[4−6] In a large reverse micelle, there is a bulk water core with bulk water observables and water molecules at the ionic surfactant interface that are very different. The orientational relaxation does decompose into a bulk water component and an interface component because the nature of large reverse micelles spatially separates the two components. The concentrated salt solutions do not have such spatial separation and are more akin to a very small reverse micelle. In the water nanopools of very small reverse micelles, virtually every water hydroxyl is interacting with the interface or, for a hydroxyl that is not interacting with the interface, it is hydrogen bonded to water molecules that are interacting with the interface. Within experimental error, for small reverse micelles, orientational relaxation behaves as a single ensemble,[5] although it is still possible to observe wavelength dependent two-component population relaxation.[52] Simulations have picked up differences in orientational dynamics in small reverse micelles depending on the proximity of the water molecule to the interface,[65] but these small differences are not observable in the IR experiments that have limitations imposed by the vibrational lifetimes.

The experiments presented here, including the orientation relaxation experiments and the 2D IR vibrational echo experiments, show that the observables, including observables of dynamics, depend mainly on the anion but also to some extent on the cation. The largest effect is on the spectrum (see Table 2). The orientational relaxation with sulfate anion does not depend on the cation within experimental error. However, the $MgBr_2$ anisotropy data for 28:1 (14:1 in bromide anion) is slower than orientational relaxation of NaBr of almost the same bromide concentration. The 2D IR vibrational echo dynamics do show a dependence on cation (see Table 3). While $MgSO_4$ and Na_2SO_4 solutions of the same concentration have identical spectral diffusion dynamics within experimental error, this is not true for other combinations of anion and cation. $MgBr_2$ and NaBr with approximately the same bromide concentration have significantly different spectral diffusion. The slowest component, which in analogy to water reflects the complete randomization of the liquid structure, is approximately a factor of 2 longer with the Mg^{2+} cation. With the sulfate anion, changing from Mg^{2+} to Na^+ does not matter, but going from Mg^{2+} to Rb^+ does matter (as seen by comparing the 56:1 solutions). With 56 waters to 1 sulfate, which is relatively dilute, the rubidium cation gives results that are not distinguishable from pure water, while the magnesium cation shows a measurable difference from pure water even at this low concentration of salt.

To reiterate an important point, different observables will have different sensitivities to the spatial nature of the system. The absorption spectrum and the population relaxation depend principally on the very local environment, particularly the nature of the hydrogen bond (ion-associated or water-associated) of the hydroxyl under observation in concentrated salt solutions. In contrast, orientational relaxation and the long time component of spectral diffusion depend on the more global rearrangement of the hydrogen bond network; therefore, the dynamics are not solely dependent on the hydrogen bond nature of a particular hydroxyl.

■ AUTHOR INFORMATION

Corresponding Author

*E-mail: fayer@stanford.edu.

Notes

The authors declare no competing financial interest.

■ ACKNOWLEDGMENTS

This work was funded by the Division of Chemical Sciences, Geosciences, and Biosciences, Office of Basic Energy Sciences of the U.S. Department of Energy through Grant # DE-FG03-84ER13251.

■ REFERENCES

(1) Laage, D.; Hynes, J. T. *Science* **2006**, *311*, 832−835.
(2) Laage, D.; Hynes, J. T. *J. Phys. Chem. B* **2008**, *112*, 14230−14242.
(3) Piletic, I. R.; Moilanen, D. E.; Spry, D. B.; Levinger, N. E.; Fayer, M. D. *J. Phys. Chem. A* **2006**, *110*, 4985−4999.
(4) Moilanen, D. E.; Fenn, E. E.; Wong, D.; Fayer, M. D. *J. Phys. Chem. B* **2009**, *113*, 8560−8568.
(5) Moilanen, D. E.; Fenn, E. E.; Wong, D.; Fayer, M. D. *J. Chem. Phys.* **2009**, *131*, 014704.
(6) Moilanen, D. E.; Fenn, E. E.; Wong, D.; Fayer, M. D. *J. Am. Chem. Soc.* **2009**, *131*, 8318−8328.
(7) Fenn, E. E.; Wong, D. B.; Fayer, M. D. *Proc. Natl. Acad. Sci. U.S.A.* **2009**, *106*, 15243−15248.
(8) Fenn, E. E.; Wong, D. B.; Giammanco, C. H.; Fayer, M. D. *J. Phys. Chem. B* **2011**, *115*, 11658−11670.
(9) Dokter, A. M.; Woutersen, S.; Bakker, H. J. *J. Chem. Phys.* **2007**, *126*, 124507.
(10) Dokter, A. M.; Woutersen, S.; Bakker, H. J. *Proc. Natl. Acad. Sci. U.S.A.* **2006**, *103*, 15355−15358.
(11) Cringus, D.; Bakulin, A.; Lindner, J.; Vohringer, P.; Pshenichnikov, M. S.; Wiersma, D. A. *J. Phys. Chem. B* **2007**, *111*, 14193−14207.
(12) Park, S.; Fayer, M. D. *Proc. Natl. Acad. Sci. U.S.A.* **2007**, *104*, 16731−16738.
(13) Fayer, M. D.; Moilanen, D. E.; Wong, D. B.; Rosenfeld, D. E.; Fenn, E. E.; Park, S. *Acc. Chem. Res.* **2009**, *42*, 1210.
(14) Fenn, E. E.; Moilanen, D. E.; Levinger, N. E.; Fayer, M. D. *J. Am. Chem. Soc.* **2009**, *131*, 5530−5539.
(15) Wong, D. B.; Sokolowsky, K. P.; El-Barghouthi, M. I.; Fenn, E. E.; Giammanco, C. H.; Sturlaugson, A. L.; Fayer, M. D. *J. Phys. Chem. B* **2012**, *116*, 5479.
(16) Kubota, J.; Furuki, M.; Goto, Y.; Kondo, J.; Wada, A.; Domen, K.; Hirose, C. *Chem. Phys. Lett.* **1993**, *204*, 273−276.
(17) Moilanen, D. E.; Piletic, I. R.; Fayer, M. D. *J. Phys. Chem. C* **2007**, *111*, 8884−8891.
(18) Sturlaugson, A. L.; Fruchey, K. S.; Fayer, M. D. *J. Phys. Chem. B* **2012**, *116*, 1777.
(19) Fecko, C. J.; Eaves, J. D.; Loparo, J. J.; Tokmakoff, A.; Geissler, P. L. *Science* **2003**, *301*, 1698−1702.
(20) Lawrence, C. P.; Skinner, J. L. *J. Chem. Phys.* **2003**, *118*, 264−272.
(21) Marcus, Y. *Chem. Rev.* **2009**, *109*, 1346−1370.
(22) Chizhik, V. I. *Mol. Phys.* **1997**, *90*, 653−660.
(23) Bakker, H. J.; Kropman, M. F.; Omata, Y.; Woutersen, S. *Phys. Scr.* **2004**, *69*, C14−C24.
(24) Kropman, M. F.; Bakker, H. J. *J. Am. Chem. Soc.* **2004**, *126*, 9135.
(25) Kropman, M. F.; Bakker, H. J. *Chem. Phys. Lett.* **2003**, *370*, 741−746.
(26) Smith, J. D.; Saykally, R. J.; Geissler, P. L. *J. Am. Chem. Soc.* **2007**, *129*, 13847−13856.
(27) Tielrooij, K. J.; Garcia-Araez, N.; Bonn, M.; Bakker, H. J. *Science* **2010**, *328*, 1006.
(28) van der Post, S. T.; Bakker, H. J. *Phys. Chem. Chem. Phys.* **2012**, *14*, 6280.
(29) Marcus, Y. *J. Solution Chem.* **2009**, *38*, 513.
(30) Woutersen, S.; Bakker, H. J. *Nature* **1999**, *402*, 507−509.
(31) Gaffney, K. J.; Piletic, I. R.; Fayer, M. D. *J. Chem. Phys.* **2003**, *118*, 2270−2278.
(32) Jansen, T. L. C.; Auer, B. M.; Yang, M.; Skinner, J. L. *J. Chem. Phys.* **2010**, *132*, 224503.
(33) Yang, M.; Li, F.; Skinner, J. L. *J. Chem. Phys.* **2011**, *135*, 164505.
(34) Rosenfeld, D. E.; Fayer, M. D. *J. Chem. Phys.* **2012**, in press.
(35) Corcelli, S.; Lawrence, C. P.; Skinner, J. L. *J. Chem. Phys.* **2004**, *120*, 8107.
(36) Park, S.; Kwak, K.; Fayer, M. D. *Laser Phys. Lett.* **2007**, *4*, 704−718.
(37) Rey, R.; Møller, K. B.; Hynes, J. T. *J. Phys. Chem. A* **2002**, *106*, 11993−11996.
(38) Lawrence, C. P.; Skinner, J. L. *J. Chem. Phys.* **2002**, *117*, 8847−8854.
(39) Badger, R. M.; Bauer, S. H. *J. Chem. Phys.* **1937**, *5*, 839.
(40) Corcelli, S.; Skinner, J. L. *J. Phys. Chem. A* **2005**, *109*, 6154−6165.
(41) Stangret, J.; Gampe, T. *J. Phys. Chem. A* **2002**, *106*, 5393.
(42) Bergström, P.-A.; Lindgren, J.; Kristiansson, O. *J. Phys. Chem.* **1991**, *95*, 8575−8580.
(43) Adams, D. M.; Blandamer, M. J.; Symons, M. C. R.; Waddington, D. *Trans. Faraday Soc.* **1971**, *67*, 611.
(44) Smiechowski, M.; Stangret, J. *Pure Appl. Chem.* **2010**, *82*, 1869.
(45) Kenkre, V. M.; Tokmakoff, A.; Fayer, M. D. *J. Chem. Phys.* **1994**, *101*, 10618.
(46) Egorov, S. A.; Berne, B. J. *J. Chem. Phys.* **1997**, *107*, 6050−6061.
(47) Steinel, T.; Asbury, J. B.; Zheng, J. R.; Fayer, M. D. *J. Phys. Chem. A* **2004**, *108*, 10957−10964.
(48) Park, S.; Moilanen, D. E.; Fayer, M. D. *J. Phys. Chem. B* **2008**, *112*, 5279−5290.
(49) Tan, H.; Piletic, I. R.; Fayer, M. D. *J. Chem. Phys.* **2005**, *122*, 174501.
(50) Moilanen, D. E.; Fenn, E. E.; Lin, Y. S.; Skinner, J. L.; Bagchi, B.; Fayer, M. D. *Proc. Natl. Acad. Sci. U.S.A.* **2008**, *105*, 5295−5300.
(51) Rezus, Y. L. A.; Bakker, H. J. *J. Chem. Phys.* **2005**, *123*, 114502.
(52) Fenn, E. E.; Wong, D. B.; Fayer, M. D. *J. Chem. Phys.* **2011**, *134*, 054512.
(53) Fayer, M. D. *Physiology* **2011**, *26*, 381−392.
(54) Lipari, G.; Szabo, A. *J. Am. Chem. Soc.* **1982**, *104*, 4546−4559.
(55) Ji, M.; Odelius, M.; Gaffney, K. J. *Science* **2010**, *328*, 1003−1005.
(56) Lipari, G.; Szabo, A. *Biophys. J.* **1980**, *30*, 489−506.
(57) Asbury, J. B.; Steinel, T.; Kwak, K.; Corcelli, S. A.; Lawrence, C. P.; Skinner, J. L.; Fayer, M. D. *J. Chem. Phys.* **2004**, *121*, 12431−12446.
(58) Asbury, J. B.; Steinel, T.; Stromberg, C.; Corcelli, S. A.; Lawrence, C. P.; Skinner, J. L.; Fayer, M. D. *J. Phys. Chem. A* **2004**, *108*, 1107−1119.
(59) Kwak, K.; Park, S.; Finkelstein, I. J.; Fayer, M. D. *J. Chem. Phys.* **2007**, *127*, 124503.
(60) Kwak, K.; Rosenfeld, D. E.; Fayer, M. D. *J. Chem. Phys.* **2008**, *128*, 204505.
(61) Schmidt, J. R.; Corcelli, S. A.; Skinner, J. L. *J. Chem. Phys.* **2005**, *123*, 044513.
(62) Schmidt, J. R.; Roberts, S. T.; Loparo, J. J.; Tokmakoff, A.; Fayer, M. D.; Skinner, J. L. *Chem. Phys.* **2007**, *341*, 143−157.
(63) Corcelli, S. A.; Lawrence, C. P.; Asbury, J. B.; Steinel, T.; Fayer, M. D.; Skinner, J. L. *J. Chem. Phys.* **2004**, *121*, 8897−8900.
(64) Miessler, G. L.; Tarr, D. A. *Inorganic Chemistry*, 3rd ed.; Pearson Prentice Hall: Upper Saddle River, NJ, 2004.
(65) Pieniazek, P. A.; Lin, Y.-S.; Chowdhary, J.; Ladanyi, B. M.; Skinner, J. L. *J. Phys. Chem. B* **2009**, *113*, 15017−15028.